Electronic supplementary information for manuscript "Global transport of perfluoroalkyl acids via sea spray aerosol"

J. H. Johansson, M. E. Salter, J-C. A. Navarro, C. Leck, E. D. Nilsson, and I. T. Cousins

Sea spray simulation chamber

All experiments were performed using a sea spray generator developed by Salter *et al.*[1] (Fig. S1). The air-flow rate was maintained and quantified using a mass flow controller (Brooks, 5851S). The slight positive pressure maintained by keeping the sweep-air flow 2 L min^{-1} higher than the sampling rate prevented contamination by the room air and excess air was vented through a flutter valve on the lid of the tank. The flow through the flutter valve was determined at the start and end of each experiment using an air flow calibrator (Gilian Gilibrator-2, Sensidyne Inc.).

In order to check for contamination within the sea spray chamber, a check for sources of particles additional to bubble bursting was conducted prior to each LPI sampling period. This involved running the sweep flow at 6 L min^{-1} with the plunging jet switched off. We then checked the number of particles larger than $\sim$ 10 nm detected using a condensation particle counter (TSI, CPC 3772) during 10 min (i.e. we operated the instrument in cumulative counting mode). Using this approach we confirmed that the particle concentration was well below 1 particle per cm^3 within the chamber (with the jet turned off) prior to each experiment.

Prior to all experiments all internal polytetrafluoroethylene-coated surfaces were rinsed thoroughly with reagent grade ethanol followed by low-organic-carbon standard deionized water (MilliQ, > 18.2 MΩcm), hereafter referred to as DIW.

Chemicals, standards and solvents

All standard compounds were purchased from Wellington Laboratories dissolved in methanol. Characterized isomeric mixtures of PFOA, PFHxS and PFOS (TPFOA, brPFHxS and TPFOS) were purchased as 50 $\mu g\,mL^{-1}$ solutions. Stable isotope-labeled and native linear PFAA standards were purchased in 2 $\mu g\,mL^{-1}$ solution mixtures (MPFAC-MXA and MPFAC-MXB respectively). The following isotope-labeled PFAAs were used as internal standards (IS): $^{13}C_4$-PFBA, $^{13}C_5$-PFPeA, $^{13}C_2$-PFHxA, $^{13}C_4$-PFHpA, $^{13}C_4$-PFOA, $^{13}C_5$-PFNA, $^{13}C_2$-PFDA, $^{13}C_2$-PFUnDA, $^{13}C_2$-PFDoDA, $^{18}O_2$-PFHxS and $^{13}C_4$-PFOS. $^{13}C_8$-PFOA was used as volumetric standard in the calculation of total method recovery of the internal standard. The isotope-labelled standards were certified to contain < 0.5 % of their native analogues.

All experiments were conducted using artificial seawater (ASW; Sigma Aldrich, S9883; manufacturer mass fraction: 55 % chloride (Cl^-), 31 % Na^+, 8 % sulfate (SO_4^{2-}), 4 % Mg^{2+}, 1 % K^+, 1 % Ca^{2+}, < 1 % other; rehydrated to an absolute salinity of 35 g kg^{-1} using DIW).

Methanol (MeOH, LiChrosolv grade), ammonium acetate (ProAnalysis) and formic acid (98 % ACS, Reag. Ph Eur) were supplied by Merck. Ammonium formiate (> 99 %, for HPLC) was purchased from Fluka. A 25 % ammonium hydroxide solution was purchased from Sigma-Aldrich.

Determination of Na^+

The concentration of Na^+ in samples was determined by chemically suppressed ion chromatography (IC; Dionex ICS-2000) using CG16/CS16 columns. A Dionex ATC-1 column was used before the injection valve to trap carbonates and other ionic contaminants. The injection volume was 25 μL. The IC-analyses were quality checked using both internal and external reference samples.[2] Systematic errors were less than 2 %. The analytical detection limit for Na^+, defined as twice the level of peak-to-peak instrument noise, was 0.02 $\mu Eq\,l^{-1}$ and the overall analytical accuracy was better than 5 %. Aliquots (1 mL) of aerosol samples were diluted 1 to 32 with DIW to bring them into the range of analysis. Bulk seawater samples were diluted 1 to 1000 with DIW into the same analytical range as the aerosol

extracts. The mean Na^+ concentration measured on each stage of the LPI for the three dynamic handling blanks was subtracted from the relevant Na^+ concentration measured in the aerosol samples.

Determination of PFCAs and PFSAs

All samples were concentrated on Oasis Weak-anion exchange (WAX) solid phase extraction (SPE) cartridges ($6\,cm^{-3}$, 150 mg, 30 μm) using a previously published method.[3] Briefly, the cartidges were preconditioned with 4.5 mL 0.3 % NH_4OH in MeOH and activated with 4.5 mL 0.1 M formic acid in DIW. After sample loading, the cartridges were washed with 5 mL 20 % MeOH in 0.1 M formic acid followed by 2 mL 0.3 % NH_4OH in DIW, before eluting the samples with 3 mL 0.3 % NH_4OH in MeOH. After the first extraction with DIW the collection foils were extracted in 2 mL MeOH in an ultrasonic bath for 15 minutes. This extract was combined with the SPE eluent and reduced to 80 μL under a gentle flow of nitrogen at 40 °C. It was then spiked with 400 pg recovery standard and diluted with 4 mM NH_4OAc to a final volume of 200 μL. Before analysis, the extracts were filtered using centrifugal filters (modified nylon 0.2 μm, 500 μL) purchased from VWR.

The final extracts corresponding to experiment A were analyzed on an Acquity ultra-performance liquid chromatography system coupled to a Xevo TQ-S tandem mass spectrometer (UPLC/MS/MS; Waters Corp.) according to a previously published method.[4] Briefly, the analytes were separated on a BEH C18 (50 × 2.1 mm, 1.7 μm particle size; Waters Corp.) analytical column using a flow rate of $0.4\,mL\,min^{-1}$ and a binary gradient of mobile phase (A) 90 % water and 10 % methanol and (B) methanol, both containing 2 mM ammonium acetate. The column was heated to 40 °C. The injection volume was 5 μL. A "PFC isolator column" obtained from Waters ("PFC kit") was inserted prior to the injector to trap and delay contamination originating from the UPLC instrument and mobile phases. The mass spectrometer was operated in negative electrospray ionization mode.

The final extracts corresponding to experiment B were analyzed on a Thermo Scientific Dionex UltiMate 3000 UHPLC coupled to a ThermoScientific TSQ Quantiva mass spectrometer, according to a previously published method.[5] Analytes were separated on an Ascentis Express F5 PFP Column (2.7 μm, 10 cm × 2.1 mm, Sigma-Aldrich) equipped with an Ascentis Express F5 PFP guard column (2.7 μm, 5.0 mm × 2.1 mm), both maintained at 30°C. An Accucore C18 (2.6 μm, 50 mm × 2.1 mm, Thermo Scientific) was placed upstream of the injector to separate PFAS originating from the LC pump from those injected onto the analytical column. The mobile phases consisted of A) 20 mM ammonium formate and 20 mM formic acid in DIW and B) MeOH. The flow was set to $0.3\,mL\,min^{-1}$. The injection volume was 25 μL. The mass spectrometer was operated in negative electrospray ionization mode. Solvent blank injections were performed to monitor sample carry over. Instrumental drift was monitored by injecting a calibration standard after every 10 injections.

PFOS was quantified using the transition to m/z 99. A linear relationship ($R^2 > 0.99$) between signal and concentration was observed for all homologues in a nine point external standard calibration curve (1/X weighted linear regression) with concentrations ranging from 0.03 to 300 $pg\,\mu l^{-1}$. The instrumental quantification limits (QLs) were defined as the lowest mass of injected standard which gave rise to a signal-to-noise ratio above 10. For PFPeA the quantification limit was defined as the lowest sample concentration which gave rise to a signal-to-noise ratio above 10. These are given in Tab. S2.

To test whether the relative response of branched and linear isomers was influenced by the mass of analyte on column, injections of TPFOA, brPFHxS and TPFOS were made in the ranges 30-7000, 28-2942 and 45-2854 respectively. The relative standard deviations observed in these tests were used to assign uncertainty to the reported percentages of branched isomers in samples (Tab. S5), as this analytical measurement error was greater than the standard deviation observed the triplicate experiments.

For individual PFOA and PFOS isomers we use the nomenclature suggested by Benskin *et al.*:[5] linear perfluorooctanoic acid (n-PFOA), perfluoro-4-methylheptanoic acid (4-PFOA), perfluoro-5-methylheptanoic acid (5-PFOA), perfluoro-6-methylheptanoic acid (6-PFOA), linear perfluorooctane sulfonic acid (n-PFOS), perfluoro-1-methylheptane sulfonic acid (1-PFOS), perfluoro-2-methylheptane sulfonic acid (2-PFOS), perfluoro-3-methylheptane sulfonic acid (3-PFOS), perfluoro-4-methylheptane sulfonic acid (4-PFOS), perfluoro-5-methylheptane sulfonic acid (5-PFOS), perfluoro-6-methylheptane sulfonic acid (6-PFOS). Perfluoro-3-methylheptanoic acid (3-PFOA) is not reported in this study, as this substance could only be detected in injections of TPFOA above 2200 pg on column. Furthermore, dimethyl-isomers of PFOA and PFOS were not included in the study as these contributed with <0.2% to ECF PFOA and PFOS.

Statistics

Statistical tests were applied to test for differences in the contribution of branched isomers in different samples in Experiment B. The data was first arcsine transformed and tested for normality using the Shapiro-Wilk test. For

PFHxS, the data from LPI stage 8 (aerosols 0.99-1.60 μm) was not normally distributed, so this data were omitted from the analysis. Levene's test did not indicate inequality of variances (p-value for means = 0.19) for PFHxS. We therefore applied a two-way ANOVA to the PFHxS data. This did not indicate that there were statistical differences in the contribution of branched isomers between sample types ($p = 0.33$). For PFOA and PFOS, Levene's test indicated inequality of variances (p-values for means were 0.022 and 0.004 respectively). We therefore applied the non-parametric Friedman test to test for differences between sample types and the Nemenyi post hoc test to investigate what samples differed from each other. For PFOA, the Friedman test indicated that there were differences between the sample types ($p = 0.0043$). The subsequent post hoc test could only detect a statistically significant difference between the SML and LPI stage 12 ($p = 0.029$, aerosols 6.57-10.16 μm). For PFOS, the Friedman test indicated that there were differences between the sample types ($p = 0.025$). The subsequent post hoc test could only detect a statistically significant difference between the bulk water and the SML ($p = 0.046$).

Additional tables

Table S1: The mean, maximum and minimum relative humidities and temperatures measured at the entrance to the LPI during each of the 6 experiments.

	Experiment A						Experiment B					
	1st replicate		2nd replicate		3rd replicate		1st replicate		2nd replicate		3rd replicate	
	RH (%)	T (°C)	RH (%)	T (°C)	RH (%)	T (°C)	RH (%)	T (°C)	RH (%)	T (°C)	RH (%)	T (°C)
Mean:	31.0	34.9	30.5	35.1	29.2	35.5	26.3	38.0	29.2	35.9	29.5	35.5
Max:	37.5	36.5	41.7	36.6	38.4	36.1	31.0	38.6	31.9	36.5	31.0	36.2
Min:	27.7	33.8	27.7	28.7	28.1	31.5	25.4	34.3	28.0	33.6	28.6	34.4

Table S2: Instrumental quantification limits of PFAAs defined as the lowest injected standard concentration which gave rise to a signal-to-noise ratio above 10.

	Instrumental quantification limit ($pg\,sample^{-1}$)	
Substance	Experiment A	Experiment B
PFPeA	3.7	
PFHxA	16	
PFHpA	3.7	
PFOA	16	6
PFNA	3.7	
PFDA	3.7	
PFUnDA	3.7	
PFDoDA	3.7	
PFTriDA	3.	
PFTeDA	3.7	
PFBS	3.3	
PFHxS	3.5	58
PFOS	3.4	58
PFDS	3.6	

Table S3: The average accuracy (%) and relative standard deviation (RSD, %) in spike-recovery tests with linear native substances (8 ng, n=3).

	Accuracy of spiked native substances (%)	
Substance	Accuracy	RSD
PFPeA	72	1
PFHxA	79	6
PFHpA	71	1
PFOA	84	3
PFNA	81	0.4
PFDA	77	6
PFUnDA	80	4
PFDoDA	76	3
PFTriDA	40	32
PFTeDA	37	32
PFBS	105	2
PFHxS	81	2
PFOS	78	8
PFDS	17	37

Table S4: The average recovery (%) of the internal standards relative to $^{13}C_8$-PFOA.

	Recovery of internal standard (%)			
	Seawater samples (n=21)		Aerosol samples (n=21)	
Substance	Average	RSD	Average	RSD
MPFPeA	109	8	106	14
MPFHxA	102	8	94	15
MPFHpA	121	7	103	13
MPFOA	95	5	90	11
MPFNA	101	11	86	14
MPFDA	88	16	80	22
MPFUnDA	63	22	65	35
MPFDoDA	60	29	68	45
MPFHxS	114	6	99	16
MPFOS	88	14	84	21

Table S5: Average ratios (and standard deviation) of individual branched isomers to corresponding linear isomer in bulk water (n=18), surface microlayer (SML, n=3) and aerosol (n=3) in Experiment B. The ratios are based on chromatographic peak areas.

	4-PFOA	5-PFOA	6-PFOA	1-PFOS	34-PFOS	5-PFOS	6-PFOS
Bulk water	0.03 (0.001)	0.11 (0.006)	0.14 (0.005)	0.13 (0.027)	0.16 (0.030)	0.19 (0.031)	0.32 (0.061)
SML	0.02 (0.004)	0.07 (0.008)	0.09 (0.012)	0.09 (0.016)	0.08 (0.013)	0.08 (0.010)	0.2 (0.038)
0.029-0.99 μm	0.02 (0.003)	0.07 (0.006)	0.10 (0.006)	0.11 (0.016)	0.15 (0.023)	0.15 (0.023)	0.27 (0.028)
0.99-1.6 μm	0.02 (0.001)	0.07 (0.005)	0.10 (0.004)	0.12 (0.013)	0.16 (0.012)	0.16 (0.036)	0.30 (0.020)
1.6-2.45 μm	0.03 (0.001)	0.09 (0.002)	0.11 (0.003)	0.14 (0.016)	0.15 (0.009)	0.13 (0.024)	0.29 (0.029)
2.45-3.96 μm	0.03 (0.000)	0.10 (0.000)	0.13 (0.004)	0.15 (0.006)	0.17 (0.006)	0.15 (0.020)	0.33 (0.021)
3.96-6.57 μm	0.03 (0.001)	0.10 (0.004)	0.13 (0.007)	0.14 (0.013)	0.17 (0.011)	0.14 (0.020)	0.33 (0.024)
6.57-10.16 μm	0.03 (0.002)	0.10 (0.007)	0.13 (0.001)	0.14 (0.011)	0.16 (0.017)	0.14 (0.026)	0.34 (0.059)
$>$ 10.16 μm	0.02 (0.000)	0.09 (0.001)	0.10 (0.000)	0.11 (0.002)	0.12 (0.007)	0.14 (0.005)	0.35 (0.030)

Table S6: Spike test for isomer analysis. Membranes were spiked to 2533, 2014 and 1982 $ng\,L^{-1}$ for PFHxS, PFOA and PFOS respectively and were subsequently extracted in 10 mL DIW to mimic LPI samples. The table displays percentage contribution of the sum of branched isomers, as well as ratios of individual branched isomers to corresponding linear isomer.

	brPFHxS (%)	brPFOA (%)	brPFOS (%)	4-PFOA	5-PFOA	6-PFOA	1-PFOS	34-PFOS	5-PFOS	6-PFOS
Mean	21	18.00	30.00	0.03	0.11	0.11	0.07	0.15	0.12	0.30
Accuracy (%)	111	115	101	118	115	107	98	100	93	97
RSD (%)	1.8	2.4	3.9	1.9	1.0	2.0	11.0	12.0	16.0	9.2

Additional figures

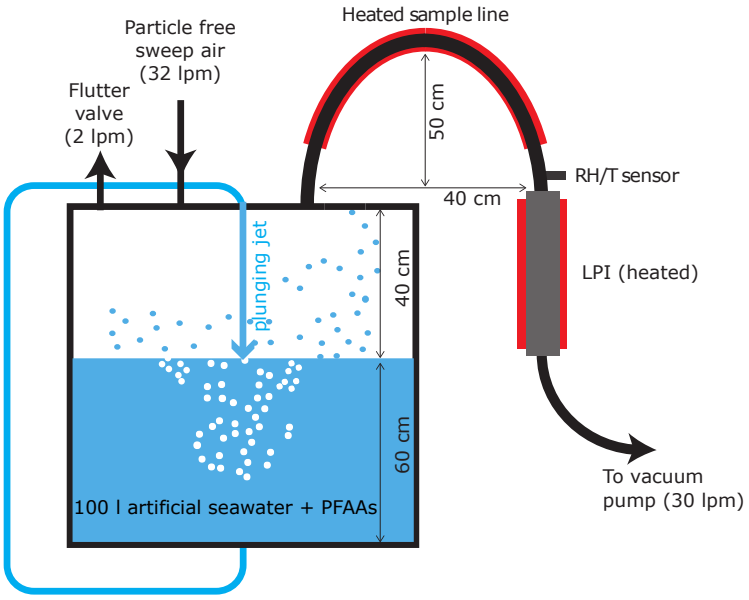

Figure S1: Schematic of the sea spray chamber used to generate nascent SSA from artifical seawater containing PFAAs. The air flow rates entering and exiting the sea spray chamber are provided in brackets.

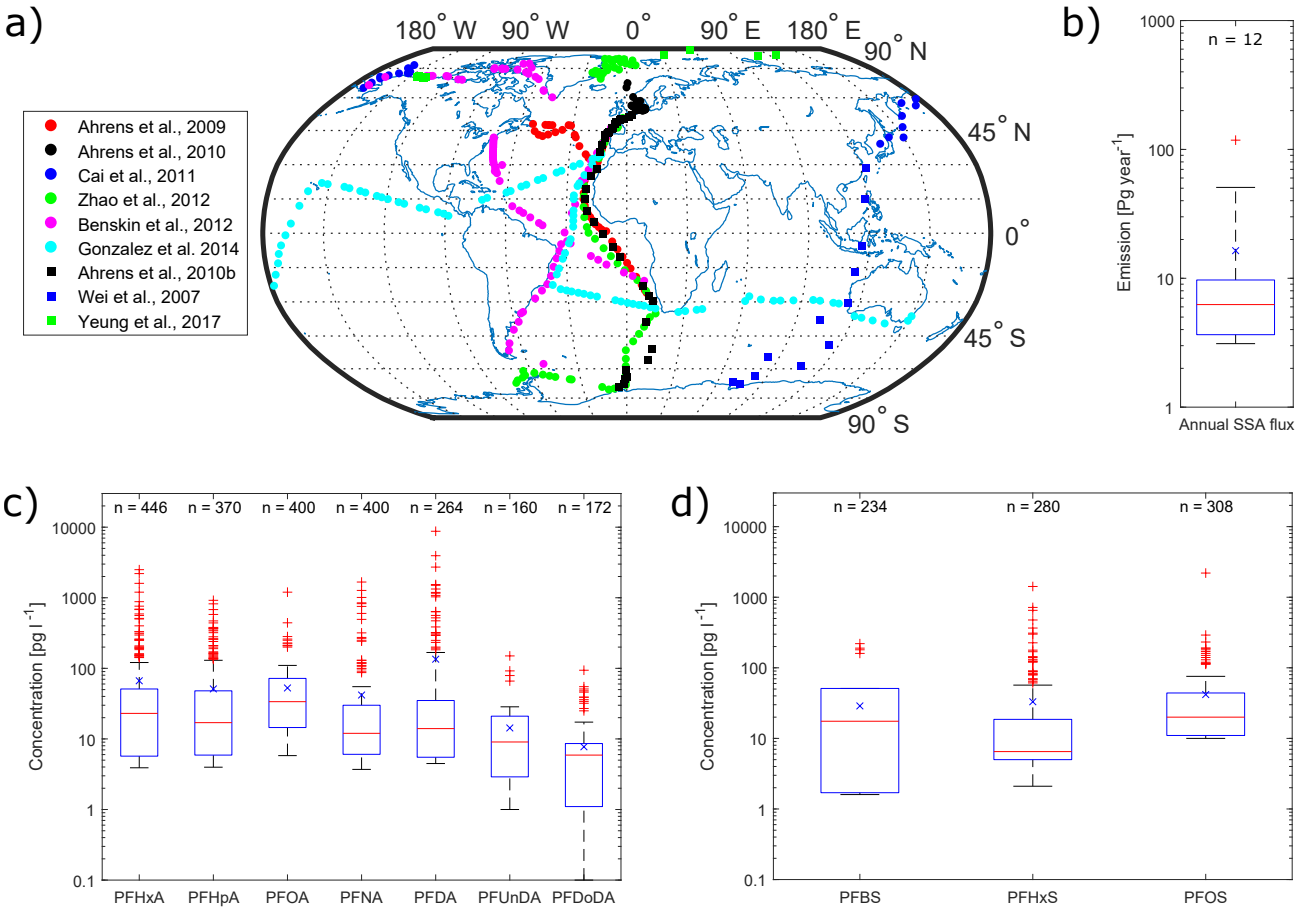

Figure S2: **(a)** The position of seawater samples collected during a series of research cruises conducted to determine PFAAs concentrations in seawater.[6;7;8;9;10;11;12;13;14] **(b)** A box and whisker plot of the global dry SSA mass emission as computed by 12 chemical transport and general circulation models participating in the AeroCom aerosol model intercomparison.[15;16] Here, the red line represents the median, the lower and upper blue boxes represent the 25th and 75th percentiles, respectively, and the whiskers represent the 10th and 90th percentiles. The blue cross represents the mean. **(c)** and **(d)** summarise the PFCA and PFSA seawater concentrations measured in the samples shown in panel a. Here, the red line represents the median, the lower and upper blue boxes represent the 25th and 75th percentiles, respectively, and the whiskers represent the 10th and 90th percentiles. The blue cross represents the mean.

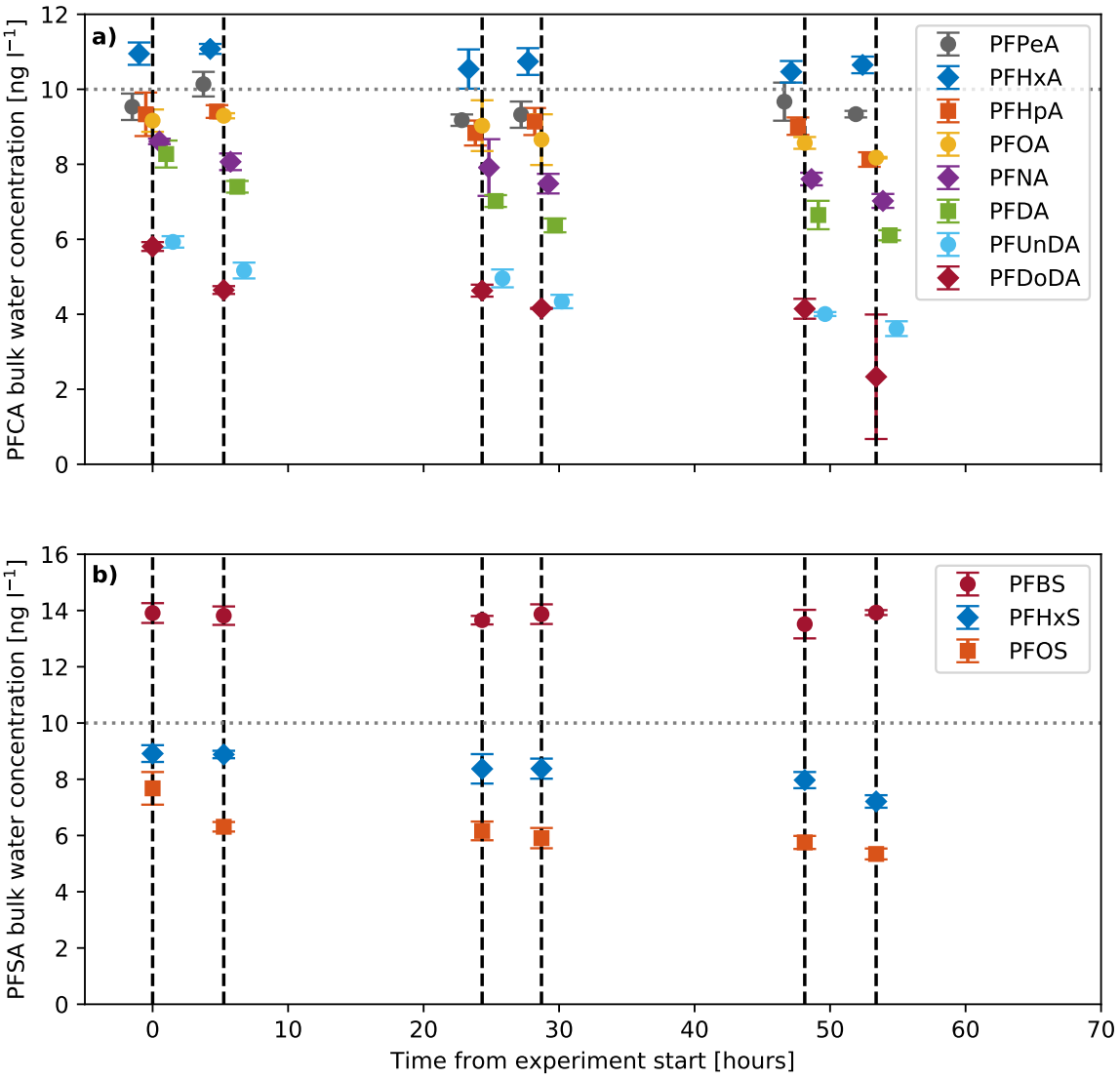

Figure S3: The temporal evolution of the bulk water concentration of **a)** perfluoroalkane carboxylic acids and **b)** perfluoroalkane sulfonic acids during the three replicates of experiment A. In **a)** the datapoints have been offset to increase visibility. Each datapoint represents the mean of triplicate samples. The dashed black lines represent the time of sample collection while the dotted grey lines represent the target concentration of our analytes.

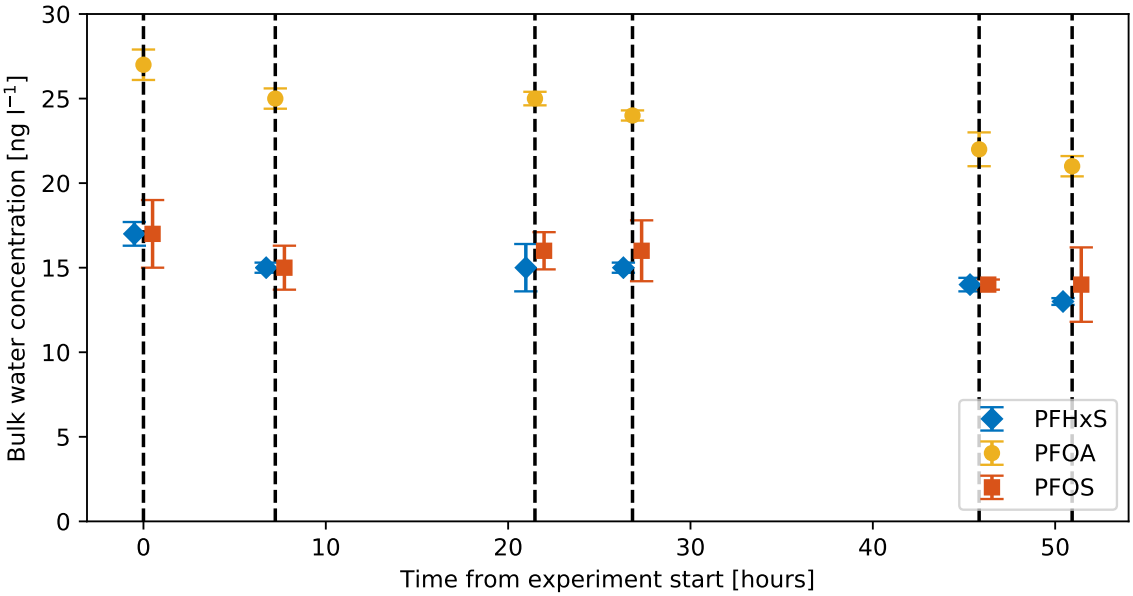

Figure S4: The temporal evolution of the bulk water concentration of PFHxS, PFOA and PFOS in Experiment B. The concentrations displayed refer to those of the linear isomers. The additional contribution from branched isomers is displayed in Fig. S11. Each datapoint represents the mean of triplicate samples. The dashed lines represent the time of sample collection.

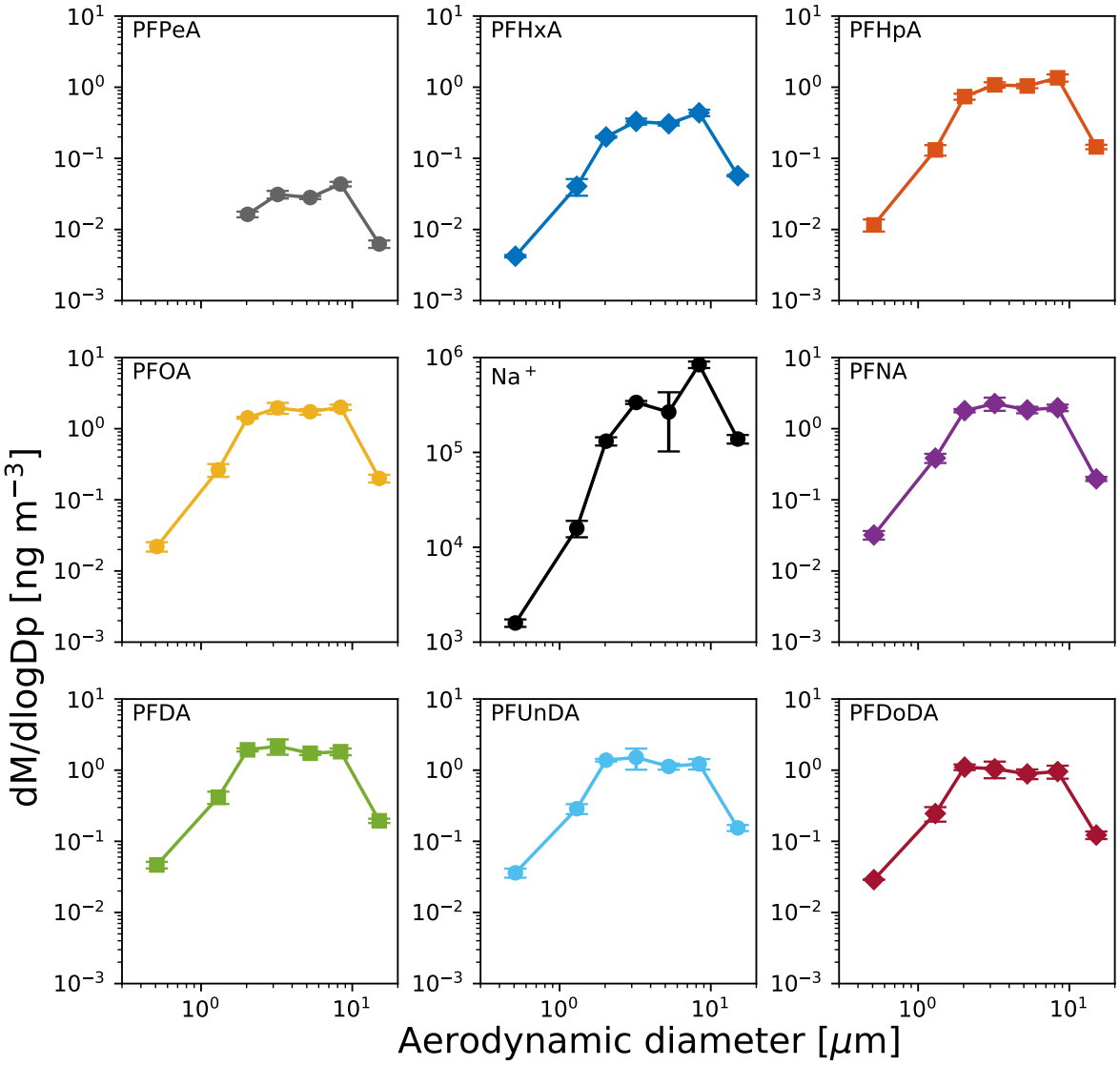

Figure S5: The aerosol mass size distribution of the measured PFCAs and Na^+ versus middle aerodynamic diameter. PFPeA was not detectable in the two lowest stages of the impactor and was below the quantification limit (14 pg sample^{-1}) in stage 13.

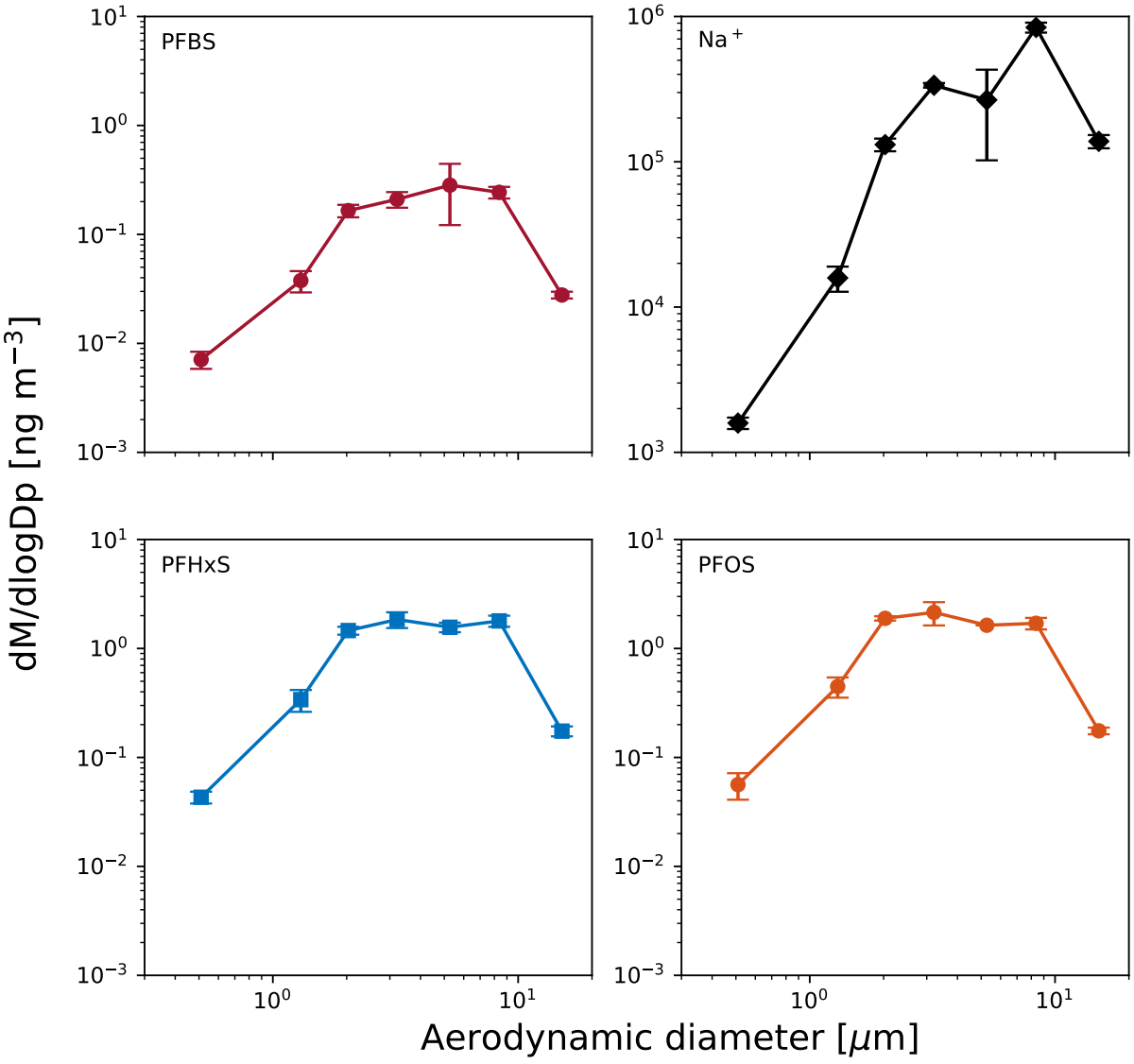

Figure S6: The aerosol mass size distribution of the measured PFSAs and Na^+ versus middle aerodynamic diameter.

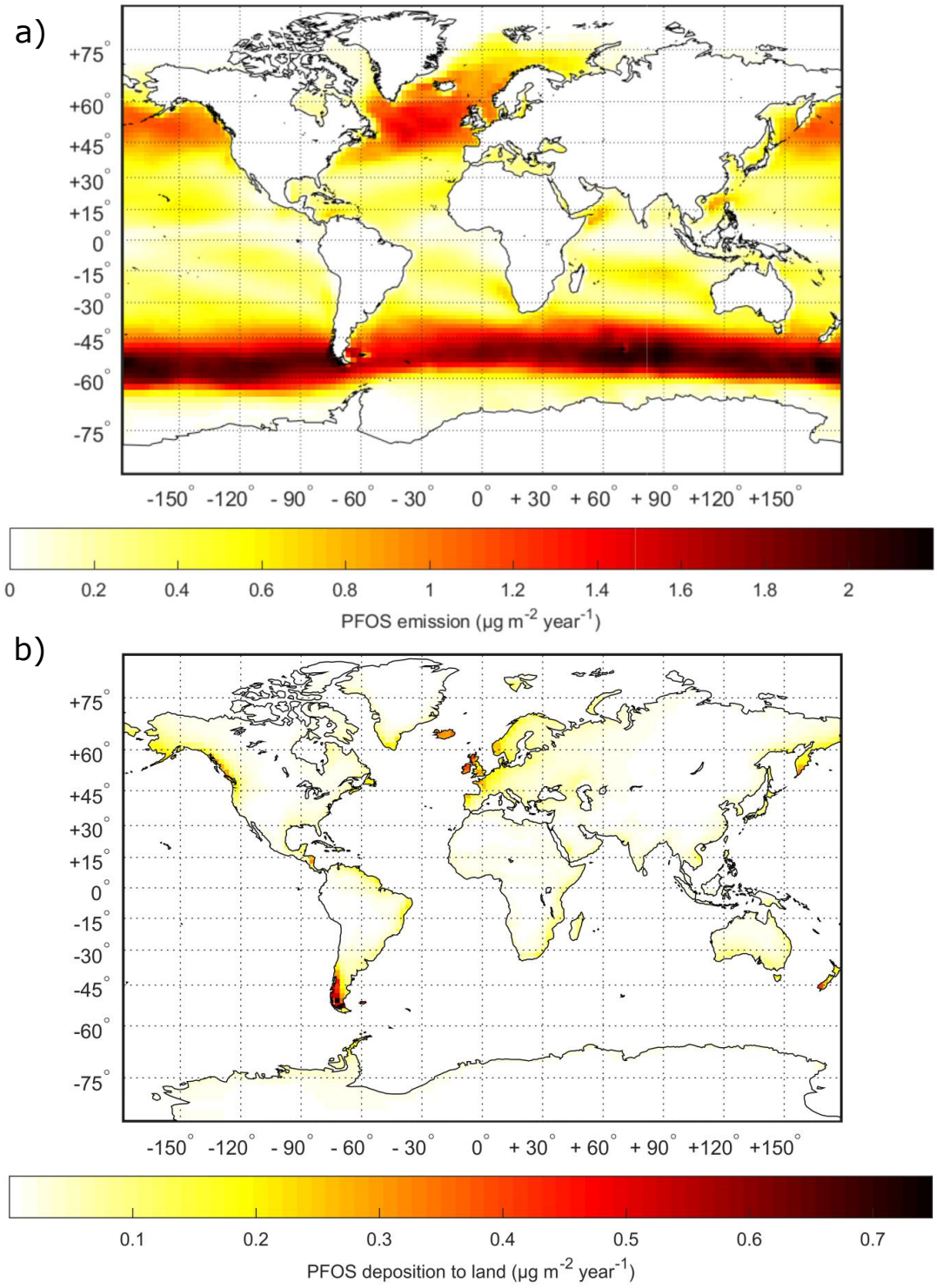

Figure S7: Global maps of **(a)** total yearly emissions of PFOS via SSA and **(b)** total yearly deposition of PFOS transported to terrestrial environments by SSA.

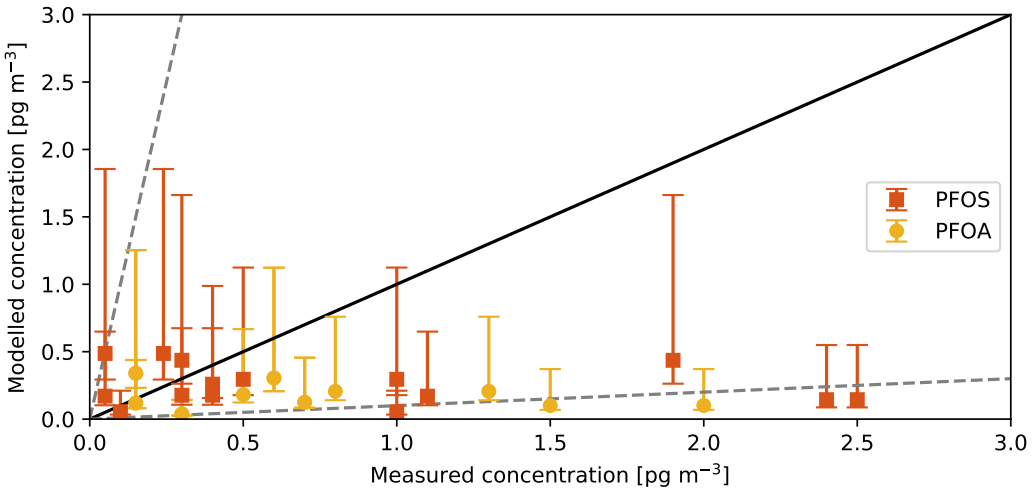

Figure S8: Comparison of model output to field data. Measured concentrations of PFOS and PFOA in air samples collected during a cruise between Germany and South Africa were reported by Jahnke *et al.*[17] Air concentrations for the corresponding dates and locations were modeled by application of measured SSA EFs corresponding to the largest mode in the model (0.99-1.60 μm), as these aerosols dominate the modelled mass of sodium. Each data point corresponds to three days.

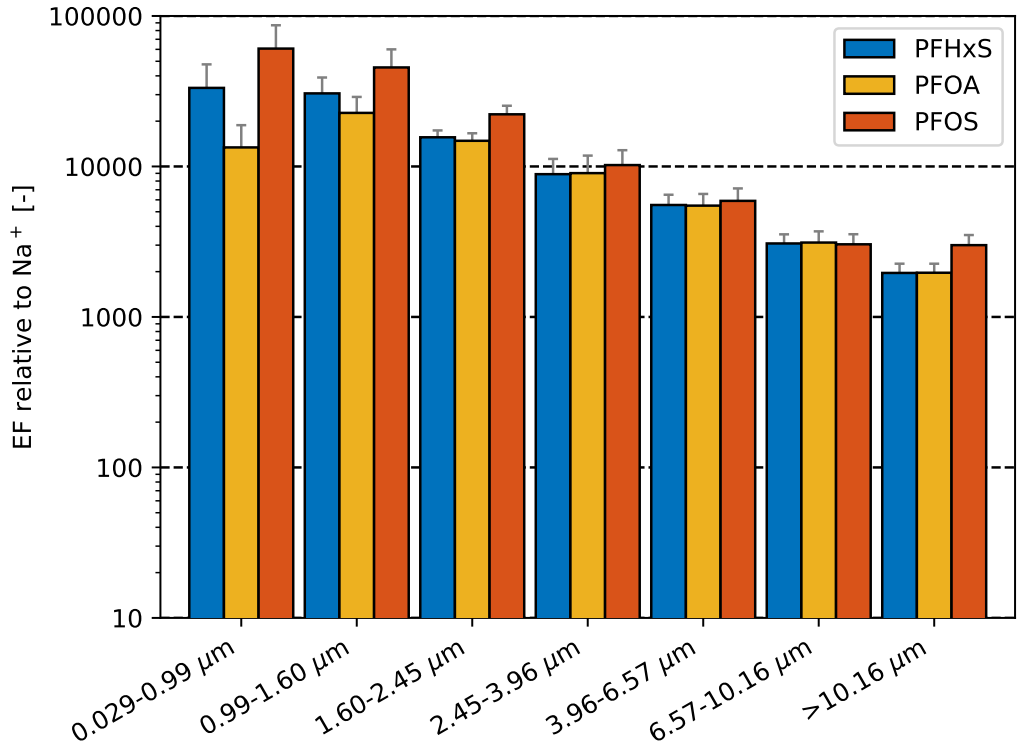

Figure S9: Aerosol enrichment factors in Experiment B (only linear isomers reported). Here error bars represent 1 standard deviation following propagation of the standard deviation of the Na^+ and PFAA concentrations measured in the seawater and aerosol samples.

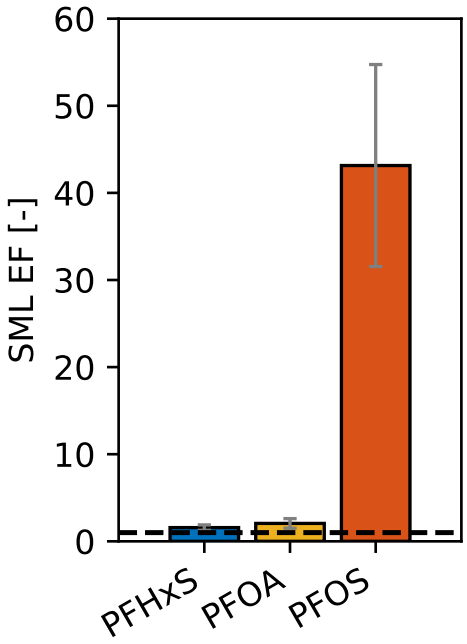

Figure S10: SML EFs in Experiment B (only linear isomers reported). Here error bars represent 1 standard deviation and the dashed line represents an enrichment factor of 1.

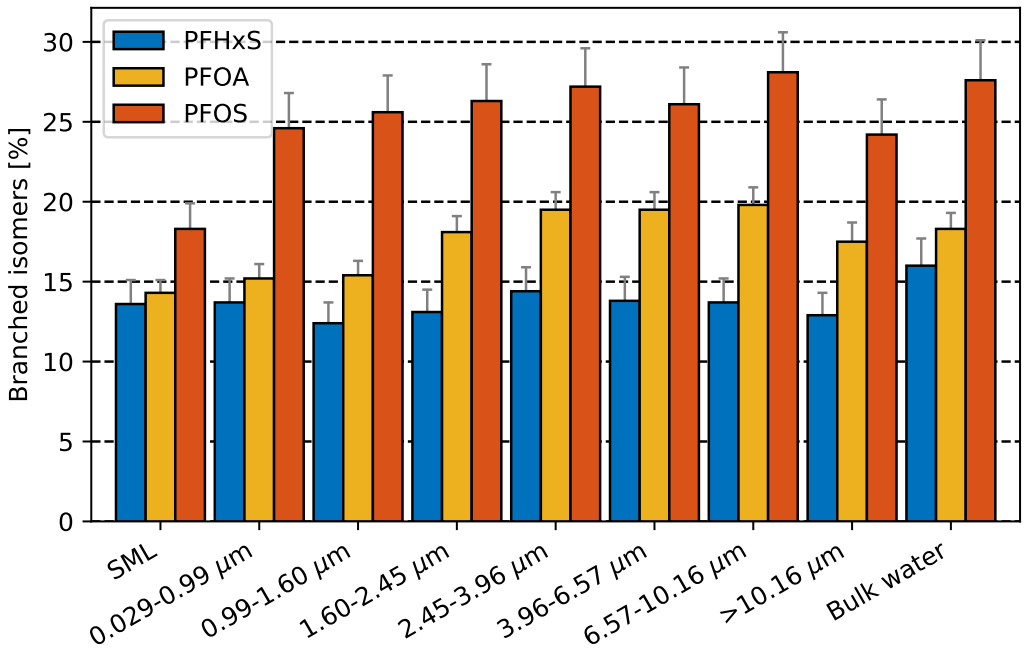

Figure S11: Contribution of the sum of branched isomers (%) to the overall concentration of PFOA, PFHxS and PFOS in Experiment B. The error bars represent the analytical measurement error, as this was greater than the standard deviation from the triplicate experiments.

Additional references

[1] M. E. Salter, E. D. Nilsson, A. Butcher and M. Bilde, On the seawater temperature dependence of the sea spray aerosol generated by a continuous plunging jet, *Journal of Geophysical Research Atmospheres*, 2014, **119**, 9052–9072.

[2] EANET, *Report of the Inter-laboratory Comparison Project 2007*, 2008.

[3] J. Löfstedt Gilljam, J. Leonel, I. T. Cousins and J. P. Benskin, Is Ongoing Sulfluramid Use in South America a Significant Source of Perfluorooctanesulfonate (PFOS)? Production Inventories, Environmental Fate, and Local Occurrence, *Environmental Science and Technology*, 2016, **50**, 653–659.

[4] R. Vestergren, S. Ullah, I. T. Cousins and U. Berger, A matrix effect-free method for reliable quantification of perfluoroalkyl carboxylic acids and perfluoroalkane sulfonic acids at low parts per trillion levels in dietary samples, *Journal of Chromatography A*, 2012, **1237**, 64–71.

[5] J. P. Benskin, M. G. Ikonomou, M. B. Woudneh and J. R. Cosgrove, Rapid characterization of perfluoralkyl carboxylate, sulfonate, and sulfonamide isomers by high-performance liquid chromatography-tandem mass spectrometry, *Journal of Chromatography A*, 2012, **1247**, 165–170.

[6] L. Ahrens, J. L. Barber, Z. Xie and R. Ebinghaus, Longitudinal and latitudinal distribution of perfluoroalkyl compounds in the surface water of the Atlantic Ocean, *Environmental Science and Technology*, 2009, **43**, 3122–3127.

[7] L. Ahrens, W. Gerwinski, N. Theobald and R. Ebinghaus, Sources of polyfluoroalkyl compounds in the North Sea, Baltic Sea and Norwegian Sea: Evidence from their spatial distribution in surface water, *Marine Pollution Bulletin*, 2010, **60**, 255–260.

[8] L. Ahrens, Z. Xie and R. Ebinghaus, Distribution of perfluoroalkyl compounds in seawater from Northern Europe, Atlantic Ocean, and Southern Ocean, *Chemosphere*, 2010, **78**, 1011–1016.

[9] M. Cai, Z. Zhao, Z. Yin, L. Ahrens, P. Huang, M. Cai, H. Yang, J. He, R. Sturm, R. Ebinghaus and Z. Xie, Occurrence of perfluoroalkyl compounds in surface waters from the North Pacific to the Arctic Ocean, *Environmental Science and Technology*, 2012, **46**, 661–668.

[10] Z. Zhao, Z. Xie, A. Möller, R. Sturm, J. Tang, G. Zhang and R. Ebinghaus, Distribution and long-range transport of polyfluoroalkyl substances in the Arctic, Atlantic Ocean and Antarctic coast, *Environmental Pollution*, 2012, **170**, 71–77.

[11] J. P. Benskin, D. C. G. Muir, B. F. Scott, C. Spencer, A. O. De Silva, H. Kylin, J. W. Martin, A. Morris, R. Lohmann, G. Tomy, B. Rosenberg, S. Taniyasu and N. Yamashita, Perfluoroalkyl acids in the atlantic and Canadian arctic oceans, *Environmental Science and Technology*, 2012, **46**, 5815–5823.

[12] B. González-Gaya, J. Dachs, J. L. Roscales, G. Caballero and B. Jiménez, Perfluoroalkylated Substances in the Global Tropical and Subtropical Surface Oceans, *Environmental Science & Technology*, 2014, **48**, 13076–13084.

[13] S. Wei, L. Q. Chen, S. Taniyasu, M. K. So, M. B. Murphy, N. Yamashita, L. W. Y. Yeung and P. K. S. Lam, Distribution of perfluorinated compounds in surface seawaters between Asia and Antarctica, *Marine Pollution Bulletin*, 2007, **54**, 1813–1818.

[14] L. W. Yeung, C. Dassuncao, S. Mabury, E. M. Sunderland, X. Zhang and R. Lohmann, Vertical Profiles, Sources, and Transport of PFASs in the Arctic Ocean, *Environmental Science & Technology*, 2017, **51**, 6735–6744.

[15] C. Textor, M. Schulz, S. Guibert, S. Kinne, Y. Balkanski, S. Bauer, T. Berntsen, T. Berglen, O. Boucher, M. Chin, F. Dentener, T. Diehl, R. Easter, H. Feichter, D. Fillmore, S. Ghan, P. Ginoux, S. Gong, A. Grini, J. Hendricks, L. Horowitz, P. Huang, I. Isaksen, I. Iversen, S. Kloster, D. Koch, A. Kirkevåg, J. E. Kristjansson, M. Krol, A. Lauer, J. F. Lamarque, X. Liu, V. Montanaro, G. Myhre, J. Penner, G. Pitari, S. Reddy, O. Seland, P. Stier, T. Takemura and X. Tie, Analysis and quantification of the diversities of aerosol life cycles within AeroCom, *Atmospheric Chemistry and Physics*, 2006, **6**, 1777–1813.

[16] G. de Leeuw, E. Andreas, M. Anguelova, C. Fairall, R. Ernie, C. O'Dowd, M. Schulz and S. Schwartz, Production Flux of Sea-Spray Aerosol, *Reviews of Geophysics*, 2011, **49**, 1–39.

[17] A. Jahnke, U. Berger, R. Ebinghaus and C. Temme, Latitudinal gradient of airborne polyfluorinated alkyl substances in the marine atmosphere between Germany and South Africa (53?? N-33?? S), *Environmental Science and Technology*, 2007, **41**, 3055–3061.